NACA RM No. L8K17a

NACA

RESEARCH MEMORANDUM

CONTROL EFFECTIVENESS AND HINGE-MOMENT MEASUREMENTS AT A MACH NUMBER OF 1.9 OF A NOSE FLAP AND TRAILING-EDGE FLAP ON A HIGHLY TAPERED LOW-ASPECT-RATIO WING

By

D. William Conner and Meade H. Mitchell, Jr.

Langley Aeronautical Laboratory
Langley Field, Va.

CLASSIFIED DOCUMENT

This document contains classified information affecting the National Defense of the United States within the meaning of the Espionage Act, USC 50:31 and 32. Its transmission or the revelation of its contents in any manner to an unauthorized person is prohibited by law. Information so classified may be imparted only to persons in the military and naval services of the United States, appropriate civilian officers and employees of the Federal Government who have a legitimate interest therein, and to United States citizens of known loyalty and discretion who of necessity must be informed thereof.

NATIONAL ADVISORY COMMITTEE FOR AERONAUTICS

WASHINGTON

January 10, 1949

NATIONAL ADVISORY COMMITTEE FOR AERONAUTICS

RESEARCH MEMORANDUM

CONTROL EFFECTIVENESS AND HINGE-MOMENT MEASUREMENTS AT A MACH NUMBER OF 1.9 OF A NOSE FLAP AND TRAILING-EDGE FLAP ON A HIGHLY TAPERED LOW-ASPECT-RATIO WING

By D. William Conner and Meade H. Mitchell, Jr.

SUMMARY

Nose flaps and trailing-edge flaps were tested on a halfspan wing model in the Langley 9- by 12-inch supersonic blowdown tunnel in the low angle-of-attack range at a Mach number of 1.9 and a Reynolds number of 3,000,000. The wing had an aspect ratio of 1.06, taper ratio of 0.31, and had airfoil sections composed of a thin flat-plate center section with the nose and trailing-edge contours formed by the wedge profiles of full-span constant chord flaps. All tests were made in the presence of a half fuselage.

The nose flap was effective in reducing the pitching moment associated with trailing-edge-flap deflection. The nose flap appeared to have about the same lift-producing effectiveness as did the trailing-edge flap. The maximum lift-drag ratio was decreased when the nose flap was deflected up and was unchanged when the trailing-edge flap was deflected down. The flap hinge moments caused by nose-flap deflection had approximately twice the magnitude of the hinge moments caused by trailing-edge-flap deflection. The rate of change of flap hinge moment with wing angle of attack was about constant for the nose flap but varied in value for the trailing-edge flap. The value for the trailing-edge flap increased negatively with increasing angle of attack and with increasing deflection of the trailing-edge flap and, for the conditions investigated, ranged from 5 percent to 37 percent of the corresponding (constant) value for the nose flap. Such a wide variation in the relationship between the hinge-moment characteristics of the two flaps would limit any attempt to effectively reduce the control force by interlinking the flaps of this configuration in a fixed linkage ratio. The nose-flap hinge moments calculated from second-order supersonic wing theory were in reasonable agreement with the experimental values.

INTRODUCTION

One of the problems confronting the designer of supersonic aircraft concerns the selection of a wing-flap combination which will provide adequate lateral control at all speeds, and yet will not have prohibitively high drag. From the free-flight investigation of reference 1, it was found that the rolling effectiveness of a full-span trailing-edge flap was improved through the transonic and low supersonic range when the wing aspect ratio was reduced, taper ratio was decreased, sweep angle of the flap elements was increased, or the airfoil-section thickness-ratio was decreased. Fortunately, most of these items have a favorable effect in minimizing the supersonic wave drag. It appears that a thin, low-aspect-ratio wing with a high amount of taper not only has most of the desirable features for realizing adequate lateral control and low drag, but also offers a practical structural arrangement. A wing of such geometry was accordingly chosen for a flap investigation at a Mach number of 1.90 in the Langley 9- by 12-inch supersonic blowdown tunnel.

In addition to a conventional trailing-edge flap, a full-span nose flap was incorporated in the half-span wing model. Nose flaps have been considered as a means of increasing maximum lift or controlling the stall at low speeds and for reducing wing twist or balancing out part of the trailing-edge-flap hinge moments at supersonic speeds. A free-flight rocket investigation of nose-flap effectiveness is reported in reference 2. Hinge moments were obtained for both a nose flap and a trailing-edge flap at a Mach number of 1.93 in the Langley 9-inch supersonic tunnel (reference 3) on a wing having an aspect ratio of 3.14 and a taper ratio of 0.59. The wing used in the present investigation had an aspect ratio of 1.06 and a taper ratio of 0.31. Reported herein are the results of this investigation, which include lift, drag, and pitching- and rolling-moment coefficients for the wing and hinge-moment coefficients for both the nose flap and trailing-edge flap. All tests were made in the presence of a fuselage.

SYMBOLS

C_L lift coefficient $\left(\frac{\text{Lift}}{qS'}\right)$

C_D drag coefficient $\left(\frac{\text{Drag}}{qS'}\right)$

C_m pitching-moment coefficient

$$\left(\frac{\text{Pitching moment about center of area}}{qS'\bar{c}}\right)$$

C_{l_g} gross rolling-moment coefficient

$$\left(\frac{\text{Gross rolling moment about axis of fuselage}}{2qS'b}\right)$$

C_{h_n} hinge-moment coefficient of nose flap

$$\left(\frac{\text{Moment about hinge axis of nose flap}}{2q \text{ moment of flap area about hinge axis}}\right)$$

C_{h_f} hinge-moment coefficient of trailing-edge flap

$$\left(\frac{\text{Moment about hinge axis of trailing-edge flap}}{2q \text{ moment of flap area about hinge axis}}\right)$$

q free-stream dynamic pressure

S' exposed semispan wing area (7.20 sq. in.)

$\bar{c}$ mean aerodynamic chord of exposed wing area (4.27 in.)

b twice the distance from fuselage axis to wing tip (4.954 in.)

α angle of attack measured with respect to free-stream direction

δ_n nose-flap deflection, measured in plane normal to hinge axis (positive when leading edge is above chord plane)

δ_f trailing-edge-flap deflection, measured in plane normal to hinge axis (positive when trailing edge is below chord plane)

R Reynolds number, based on $\bar{c}$

M Mach number

MODEL

A photograph of the half-span flapped wing model is presented in figure 1. The principal dimensions of the configuration are shown in figure 2. The steel wing and brass fuselage had polished surfaces.

The wing had a 45° sweptback leading edge and a 45° sweptforward trailing edge. The aspect ratio was 1.06, and the taper ratio was 0.31, based upon wing dimensions obtained by extending the leading and trailing edges to the axis of the fuselage. The main wing panel was a flat plate, and the resulting wing thickness ratio equaled 3.4 percent chord at the

fuselage juncture and 9 percent chord at the wing tip. Attached to the main wing panel were full-span constant-chord nose and trailing-edge flaps. The flap cross sections were wedge shaped with an included wedge angle of 11.5° measured streamwise. The constant chord of each flap amounted to 17 percent of the wing chord at the fuselage juncture, or approximately 45 percent of the tip chord. As shown in figure 2, the outboard ends of the flap and wing were modified to simulate a configuration using outboard flap hinge bearings. The flaps were attached to the main wing panel with full-span plates fitted in grooves on the wing chord plane. A range of flap deflections was obtained through the use of interchangeable plates, each bent to a given deflection. The bend line lay along the flap hinge line. This arrangement corresponded to a sealed flap having no overhanging balance.

TUNNEL AND TEST TECHNIQUE

The present tests were conducted in the Langley 9- by 12-inch supersonic blowdown tunnel at a free-stream Mach number of 1.9. The tunnel is of the nonreturn type and utilizes the exhaust air from the Langley 19-foot pressure tunnel. The air enters the tunnel at an absolute pressure of about $2\frac{1}{3}$ atmospheres and contains about 0.003 pound of water per pound of air.

The half-span wing model was cantilevered from the tunnel wall and was tested in the presence of a half fuselage. The half fuselage, which was shimmed out 0.25 inch from the tunnel wall, rotated through the angle-of-attack range with the wing, although no fuselage loads were measured. A discussion is given in reference 4 concerning the various factors which might cause the experimental results obtained by this test technique to differ from what would exist in the ideal case (complete model in free flight). The flat plate central panel of the wing extended through the fuselage to connect the wing with the balance. Under no load the gap between the extended central panel and the fuselage was 0.015 inch, and the gap between the overhanging portion of the wing and the fuselage was 0.005 inch. A few pressure measurements obtained on the portion of the central panel shielded from the air stream by the fuselage indicated no significant air loads. The angle-of-attack range was limited by the deflection due to aerodynamic loads.

Flap moments were measured by two electrical strain gages mounted on each surface of each attachment plate (fig. 2). The electrical centers of these gages about which the moments were measured were displaced about 0.03 inch from the bend line and the flap area moment used in calculating hinge-moment coefficients were taken around the axis of the electrical center. It was believed that hinge-moment coefficients obtained in this manner would closely approximate the true hinge-moment coefficients taken with respect to the flap hinge line. The flap

deflections have been corrected for deflection due to flap loading by means of static calibrations and measured flap hinge moments.

The dynamic pressure and test Reynolds number decreased about 3.5 percent during the course of each run because of decreasing pressure of the inlet air. The average dynamic pressure of these tests was 11.7 pounds per square inch, and the average Reynolds number was 3,000,000.

PRECISION OF DATA

Free-stream Mach number has been calibrated at 1.90 ± 0.02. This Mach number was used in determining the dynamic pressure. Calibration tests made with the tunnel clear in the space normally occupied by the model and extending about 4 inches ahead of the wing reference axis and outside the wall boundary layer indicated that static pressure varied about ± 1.5 percent from a mean value.

The accuracy of measurements is believed to be of the order indicated in the following table:

Variable	Error
α	$\pm 0.05^\circ$
δ_n and δ_f	.15
C_L	.005
C_D	.001
C_m	.001
C_{h_n} and C_{h_f}	.01
C_{l_g}	.003

RESULTS

Sizable changes in flap deflection from the no-load values were introduced by aerodynamic flap loading. As will be shown later, the trailing-edge flap had little change in loading throughout the angle-of-attack range and, therefore, had a relatively constant ($\pm 0.05^\circ$) corrected

deflection for any given configuration. The nose flap, on the other hand, had large load changes due to angle of attack and, consequently, had a variable deflection through the angle-of-attack range. A considerable number of tests were unrelated in terms of δ_f to any other tests and therefore these data could not be included in the plots and crossplots intended for use in analyzing the characteristics at constant value of nose-flap deflection. In order to present all data for constant nose-flap deflections as well as to avoid a heavy dependence on the fairing between two or three test points necessary in crossplots, the plots for constant nose-flap deflection have been derived, not from crossplots, but from the test points modified in value by means of the following procedure:

1. Each aerodynamic component was plotted against nose-flap deflections and for constant values of trailing-edge-flap deflections and for constant angles of attack. These plots are presented as part (a) of figures 3 to 7.

2. Each test point was then shifted by an increment in the coefficient which, in effect, would change the nose-flap deflection for a given test condition to a constant value through the angle-of-attack range. The shift (usually less than 1°) was to the nearest of three arbitrarily chosen deflections: 0°, 4.6°, or 8.7°. (These particular deflections allow the nose flap to be compared with the trailing-edge flap at the same flap deflections.) The increment in coefficient was calculated as the product of the increment in nose-flap deflection, and the average slope values obtained from part (a) of the figures 3 to 7. In the case of rolling-moment coefficient, the value of $dC_l/d\delta_n$ was lacking and had to be approximated from $dC_L/d\delta_n$ and an assumed fixed location of the spanwise center of pressure. The modified data were used in plotting the remaining parts of figures 3 to 7 and figures 8 and 9.

Only two to four data points were available for defining each curve of aerodynamic coefficient plotted against flap deflection (figs. 3 to 7) because of the limited number of test configurations. It was believed, therefore, that the only analysis justifiable would be one limited to determining the over-all trends and that this could best be accomplished by fairing a family of related curves for each figure (when no appreciable discrepancies exist between points of identical conditions on the faired curves of the several parts of each figure). Symbols have been used in presenting the modified data in order to show clearly the scatter in the modified data points from the faired curves. The use of symbols aids in separating the definite trends in the aerodynamic characteristics from the random test errors known to be present.

DISCUSSION

For a complete model of this wing configuration at $M = 1.90$, the trailing-edge flap on one panel would lie within the region of influence

of the nose flap on the other wing panel. Since the complementary wing panel was a mirror image of the half-span wing undergoing tests, the flap configuration in the tests simulated flaps (producing lift) on a complete model, rather than ailerons (producing rolling moment through flap deflections of the opposite sense on the two wing panels). It is believed that when the flaps act as ailerons the interference effect of the nose flap on the opposite trailing-edge flap would be small.

Lift.- Some small nonlinearities appeared to exist in the rate of change of lift coefficient with deflection of each flap (figs. 3(a) and 3(b)), though the amount of data is not considered sufficient to define any general trends in interaction effects. The average value of $dC_L/d\delta$ was 0.004 for both flaps, and when the two flaps were deflected equally (up deflection of the nose flap and down deflection of the trailing-edge flap) $dC_L/d\delta$ equalled 0.007 indicating that the lift effectiveness was almost additive. The lift coefficient varied linearily with the angle of attack for all flap combinations and had a value of $dC_L/d\alpha$ of about 0.0365. No attempt has been made to calculate the loading of this wing at this Mach number, since the Mach cone originating at the wing tip intersects the wing-fuselage juncture. It should be pointed out that the test results of reference 4 indicated that when the size of the fuselage is relatively large with respect to the wing, the wing angle of attack may be effectively increased by as much as 30 percent by the upwash field of the fuselage.

Drag.- The minimum drag coefficient for all flap combinations (fig. 4) ranged from 0.020 to 0.024, and, in general, occurred somewhere within the range of angles of attack tested. For any given positive angle of attack tested, the drag coefficient increased with increasing nose-flap deflection (fig.4(a)) but did not increase appreciably with trailing-edge-flap deflection (fig. 4(b)) until after a flap deflection of 8° was reached. At positive angles of attack the magnitude of the drag rise caused by deflecting the nose flap was unaffected by trailing-edge-flap deflection. Deflecting the trailing-edge flap in the positive angle-of-attack range caused the curve of C_D plotted against α (fig. 4(d)) to be merely displaced by a positive increment in drag coefficient. Deflecting the nose flap tended to rotate the curve with a resultant increase in the slopes along the curve and a decrease in the angle of attack for minimum drag.

In figure 4(e) a tangent from the origin to each curve of C_L plotted against C_D could be obtained or closely approximated from the faired curves for nearly all flap combinations thus making possible a a limited analysis of maximum lift-drag ratio. With flaps undeflected, the maximum value of lift-drag ratio for the wing panel was about 6. In the positive lift range value was reduced when nose flaps were deflected but was not changed when trailing-edge flap was deflected (up to $\delta_f = 8^\circ$). It should be pointed out that fuselage drag is not included, and the trends in drag for the complete wing-fuselage combination could be much different.

Pitching moment.- The value of $dC_m/d\delta_n$ obtained from the curves of figure 5(a) was independent of trailing-edge-flap deflection but decreased as the angle of attack was increased. The value of $dC_m/d\delta_f$ was independent of both nose-flap deflection and angle of attack. A nose flap would be very effective in reducing wing twist caused by trailing-edge-flap deflection. For any fixed trailing-edge-flap deflection, the amount of nose-flap deflection required to balance out the pitching moment associated with trailing-edge-flap deflection would increase with increasing angle of attack and would equal the trailing-edge-flap deflection at an angle of attack near 4°.

The positive values of $dC_m/d\alpha$ and dC_m/dC_L (figs. 5(d) and 5(e)) decreased slightly as the nose-flap deflection was increased. The chordwise aerodynamic-center location calculated from dC_m/dC_L for the flaps-neutral condition was 18 percent of the mean aerodynamic chord ahead of the center of area. Deflecting both flaps to 8.7° moved the aerodynamic-center position back about 3 percent of the mean aerodynamic chord with no appreciable trim change at zero lift.

Flap hinge moments.- The hinge-moment coefficient of the nose flap varied linearly with nose-flap deflection as shown by figure 6(a). The value of $dC_{h_n}/d\delta_n$, which was about 0.020, was little affected by either angle-of-attack change or trailing-edge-flap deflection. The data shown in figure 6(b) for two consecutive tests of a given nose-flap setting where δ_f was tested at 0° and 13° indicated that the hinge-moment coefficient of the nose flap was essentially independent of trailing-edge-flap deflection. The value of $dC_{h_n}/d\alpha$ was about 0.038 (fig. 6(c)) with some slight unsystematic variations (within the experimental accuracy) for various flap combinations.

The value of $dC_{h_n}/d\delta_n$ was calculated by the three-dimensional flat-plate theory (reference 5) to be 0.0155. When this value was corrected for thickness by using Busemann's second-order approximation theory with sections and Mach number components taken normal to the leading edge and by considering the two-dimensional thickness-effect factor to apply in the tip cone fields, the value of $dC_{h_n}/d\delta_n$ was increased to 0.0226. This value was about 10 percent higher than experiment. The flow fields on the nose flap would be the same for angle-of-attack change as for flap deflection and, therefore, the calculated $dC_{h_n}/d\alpha$ would differ from the calculated $dC_{h_n}/d\delta_n$ only by the secant of the sweep angle. The resultant calculated value of $dC_{h_n}/d\alpha$ would not include the effect of fuselage upwash. The upwash along the flap leading edge was calculated by a method recommended in reference 6; and when this was applied to the span-load distribution of the flap, the value of $dC_{h_n}/d\alpha$ was increased to 0.037, which was slightly lower than the experimental value of 0.038. It should be pointed out that theory assumes an attached shock wave; whereas, the

angle at which the shock detaches for the Mach component normal to the wing leading edge is slightly less than the wedge half angle of this flap profile.

As shown in figure 7(a), the hinge-moment coefficient for the trailing-edge flap became more positive with increasing nose-flap deflection in the negative angle-of-attack range. The magnitude of this effect diminished with increased angle-of-attack until at $\alpha = 3.75^{\circ}$, the highest investigated, the value of C_{h_f} tended to be independent of nose-flap deflection. The trailing-edge flap hinge-moment coefficient varied almost linearly with trailing-edge-flap deflection (fig. 7(b)), with the value of $dC_{h_f}/d\delta_f$ becoming slightly more negative with increasing angle of attack. The average value of $dC_{h_f}/d\delta_f$ was about -0.010. The rate of change of C_{h_f} with angle of attack, shown in figure 7(d), increased negatively with angle of attack and with deflection of the trailing-edge flap. In the positive angle-of-attack range increasing the trailing-edge-flap deflection from 0° to 13° increased negatively $dC_{h_f}/d\alpha$ from -0.002 to -0.009 for $\delta_n = 0^{\circ}$ and from -0.006 to -0.014 for $\delta_n = 8.7^{\circ}$.

Since the hinge moments caused by nose-flap deflection were about twice those caused by trailing-edge-flap deflection, a fixed linkage ratio (equal to $\sqrt{2}$) between the flaps would practically balance out the control force required for flap deflection. Neither this nor any other fixed linkage ratio would, however, be universally effective in balancing out hinge moments caused by angle-of-attack change because of the large variation in the value of $dC_{h_f}/d\alpha$ (which ranged from about 5 to 37 percent of the constant values of $dC_{h_n}/d\alpha$). As a matter of interest, the hinge-moment measurements of reference 3, which were obtained at about the same Mach number but on a wing having less taper, higher aspect ratio, and no fuselage, indicated that nose-flap hinge moments due to both angle of attack and flap deflection were three times as large as the corresponding hinge moments for the trailing-edge flap, and a linkage system appeared feasible.

Rolling-moment characteristics.- After completing tests on this model, the balance system was altered to include measurements of rolling moment. The roll component of the balance was designed for models having values of wing span and area several times those for this model. As a result, when rolling-moment characteristics were obtained from additional tests of this model, the accuracy between test configurations was not of a sufficient degree for quantitative analysis of flap rolling effectiveness. There was, however, a consistency in the rate of change of gross rolling moment with angle of attack $\left(dC_{l_g}/d\alpha\right)$ for the various flap combinations. From the data of figure 8 an average value for $dC_{l_g}/d\alpha$ of -0.0053 was obtained. From this value and a value of $dC_L/d\alpha = 0.0365$, the spanwise center-of-pressure location of the exposed panel was calculated to be $0.58\frac{b}{2}$ from the fuselage center line. This distance is the same as that to the spanwise center of area of the exposed panel.

Fuselage length.- A few tests were made in which the distance from the nose of the fuselage to the midpoint of the wing was increased by 24 percent. The results shown in figure 9 indicate that locating the wing farther back on the constant diameter section of the fuselage had no noticeable effect on the aerodynamic characteristics of the wing.

Unsealed flap.- The plate used in obtaining $\delta_f = 4.6^\circ$ was slotted along the bend line to determine any effects of unsealing the flap. The leading edge of the flap was cut away to vary the width of the gap between the wing panel and the flap by amounts ranging from 1 to 7 percent of the flap chord. The data are not presented since there was no appreciable effect on the measured aerodynamic characteristics of either the flap or the wing. A test with the wing reversed on the fuselage showed that the 7-percent slot in the flap did not change the hinge-moment characteristics of the flap acting as a nose flap at that flap deflection.

CONCLUSIONS

From tests at a Mach number of 1.9 of a trapezoidal low-aspect-ratio wing with a nose flap and trailing-edge flap in the Langley 9- by 12-inch supersonic blowdown tunnel, the following conclusions may be drawn:

1. Deflecting the nose flap was an effective means of reducing the pitching moment associated with the trailing-edge-flap deflection. For any fixed trailing-edge-flap deflection, the amount of nose-flap deflection required increased with increasing angle of attack and would equal the trailing-edge-flap deflection at an angle of attack near 4°.

2. The nose flap appeared to have about the same lift-producing effectiveness as did the trailing-edge flap. The maximum lift-drag ratio was decreased when the nose flap was deflected and was unchanged when the trailing-edge flap was deflected.

3. The flap hinge moments caused by nose-flap deflection had twice the magnitude of the hinge moments caused by trailing-edge-flap deflection. The rate of change of flap hinge moment with wing angle of attack was constant for the nose flap but varied in value for the trailing-edge flap. The value for the trailing-edge flap increased negatively with increasing angle of attack and with increasing deflection of the trailing-edge flap and, for the conditions investigated, ranged from 5 percent to 37 percent of the corresponding (constant) value for the nose flap. Such a wide variation in the relationship between the hinge-moment characteristics of the two flaps would limit any attempt to reduce effectively the control force by interlinking the flaps of this configuration in a fixed linkage ratio.

4. The nose-flap hinge moments calculated from second-order supersonic wing theory were in reasonable agreement with the experimental values.

Langley Aeronautical Laboratory
National Advisory Committee for Aeronautics
Langley Field, Va.

REFERENCES

1. Sandahl, Carl A., and Strass, H. Kurt: Additional Results in a Free-Flight Investigation of Control Effectiveness of Full-Span, 0.2-Chord Plain Ailerons at High Subsonic, Transonic, and Supersonic Speeds to Determine Some Effects of Wing Sweepback, Aspect Ratio, Taper, and Section Thickness Ratio. NACA RM No. L7L01, 1948.

2. Strass, H. Kurt: Free-Flight Investigation of the Rolling Effectiveness at High Subsonic, Transonic, and Supersonic Speeds of Leading-Edge and Trailing-Edge Ailerons in Conjunction with Tapered and Untapered Plan Forms. NACA RM No. L8E10, 1948.

3. Boatwright, William B., and Rainey, Robert W.: Hinge-Moment Measurements of a Wing with Leading-Edge and Trailing-Edge Flaps at a Mach Number of 1.93. NACA RM No. L8J06a, 1948.

4. Conner, D. William: Aerodynamic Characteristics of Two All-Movable Wings Tested in the Presence of a Fuselage at a Mach Number of 1.9. NACA RM No. L8H04, 1948.

5. Lagerstrom, P. A., and Graham, Martha E.: Linearized Theory of Supersonic Control Surfaces. Rep. No. SM-13060, Douglas Aircraft Co., Inc., July 24, 1947.

6. Beskin, L.: Determination of Upwash around a Body of Revolution at Supersonic Velocities. CVAC-DEVF Memo. BB-6, APL/JHU-CM-251, The Johns Hopkins Univ., Appl. Phys. Lab., May 27, 1946.

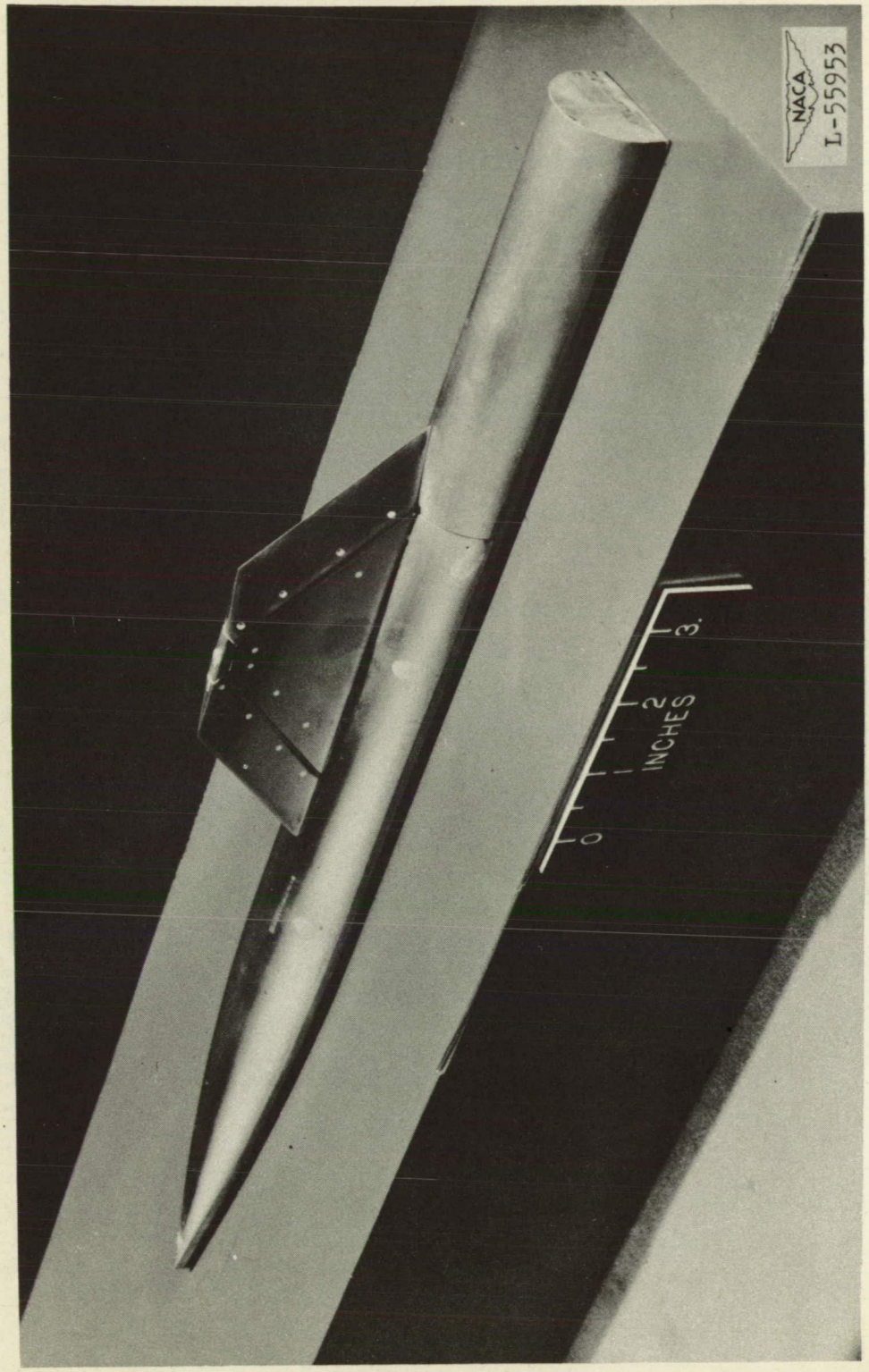

Figure 1.- Flapped wing model.

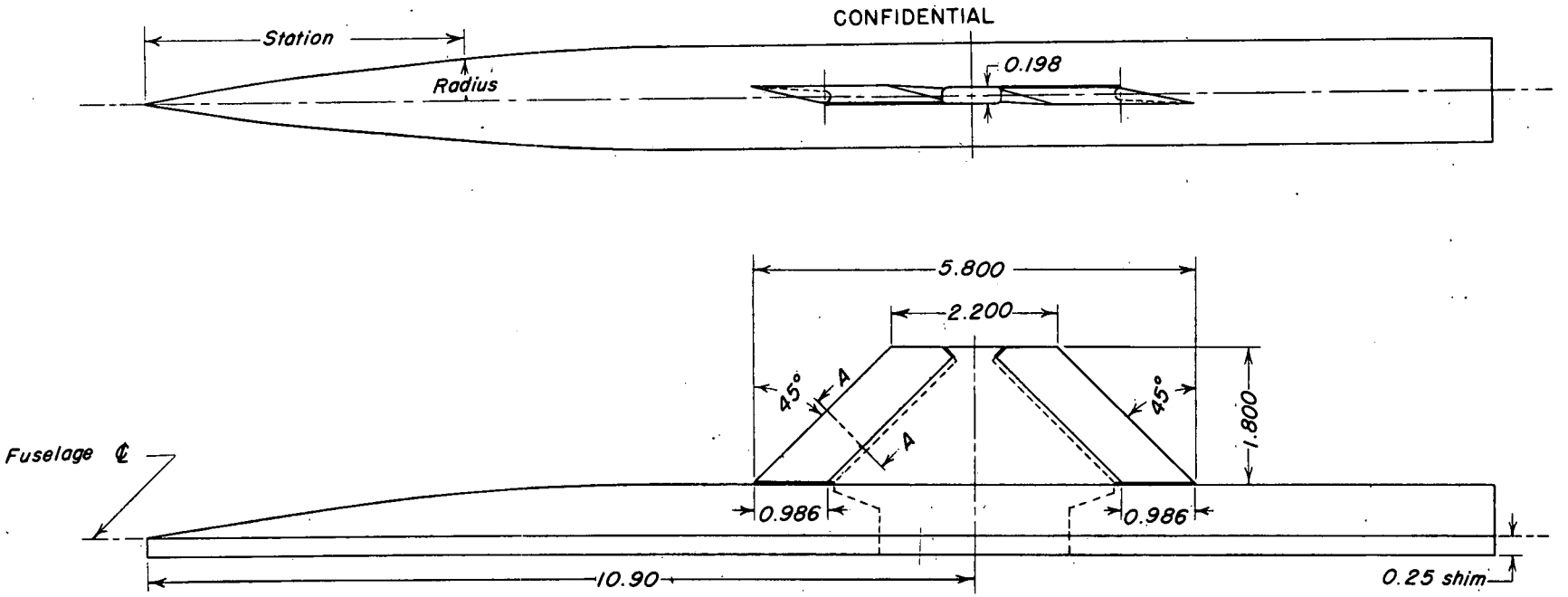

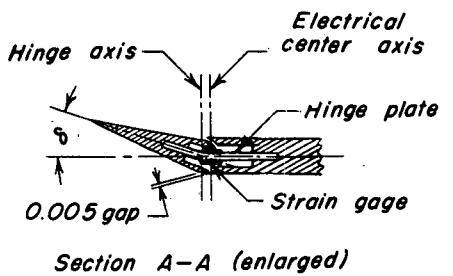

FUSELAGE ORDINATES			
Station	Radius	Station	Radius
0	0	4.74	0.613
.68	.119	5.41	.650
1.35	.226	6.09	.672
2.03	.325	6.77	.677
2.71	.413	↓	↓
3.38	.490	↓	↓
4.06	.555	17.82	.677

NACA

Figure 2.- Details of flapped wing model; mean aerodynamic chord, 4.27; span, 4.95. All dimensions in inches.

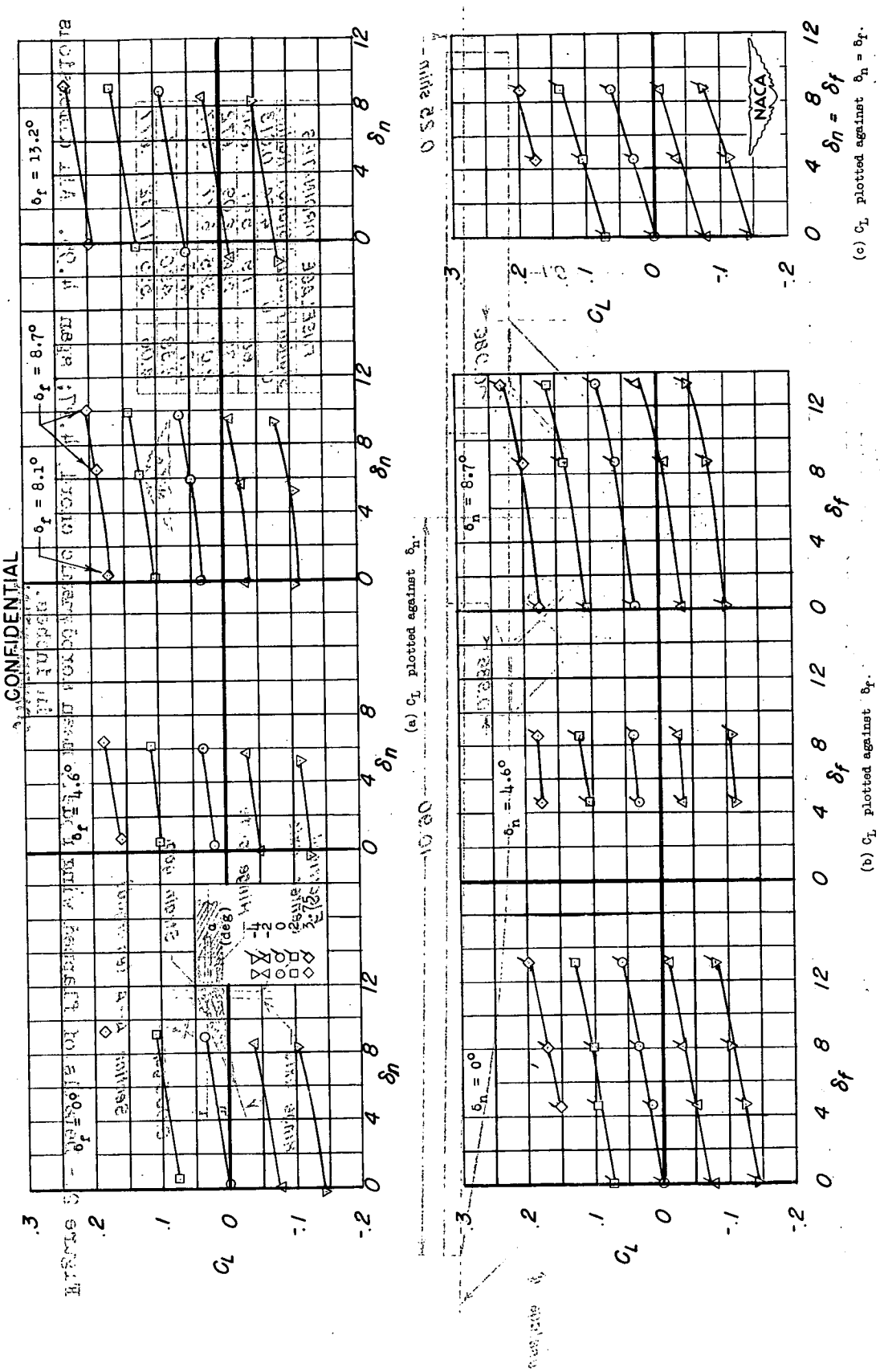

(a) C_L plotted against δ_n.

(b) C_L plotted against δ_f.

(c) C_L plotted against $\delta_n = \delta_f$.

Figure 3.- Lift characteristics of flapped wing tested in the presence of a fuselage. R = 3.0 × 10^6; M = 1.9. Flagged symbols indicate modified test data.

CONFIDENTIAL

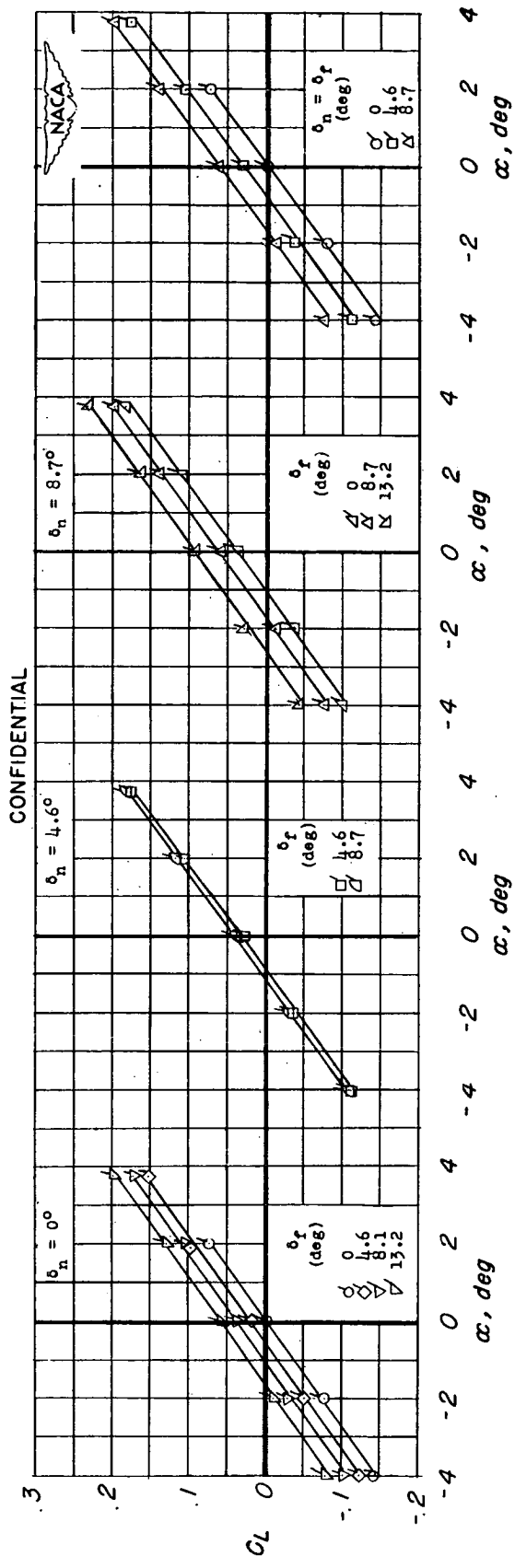

(d) C_L plotted against α.

Figure 3.- Concluded.

CONFIDENTIAL

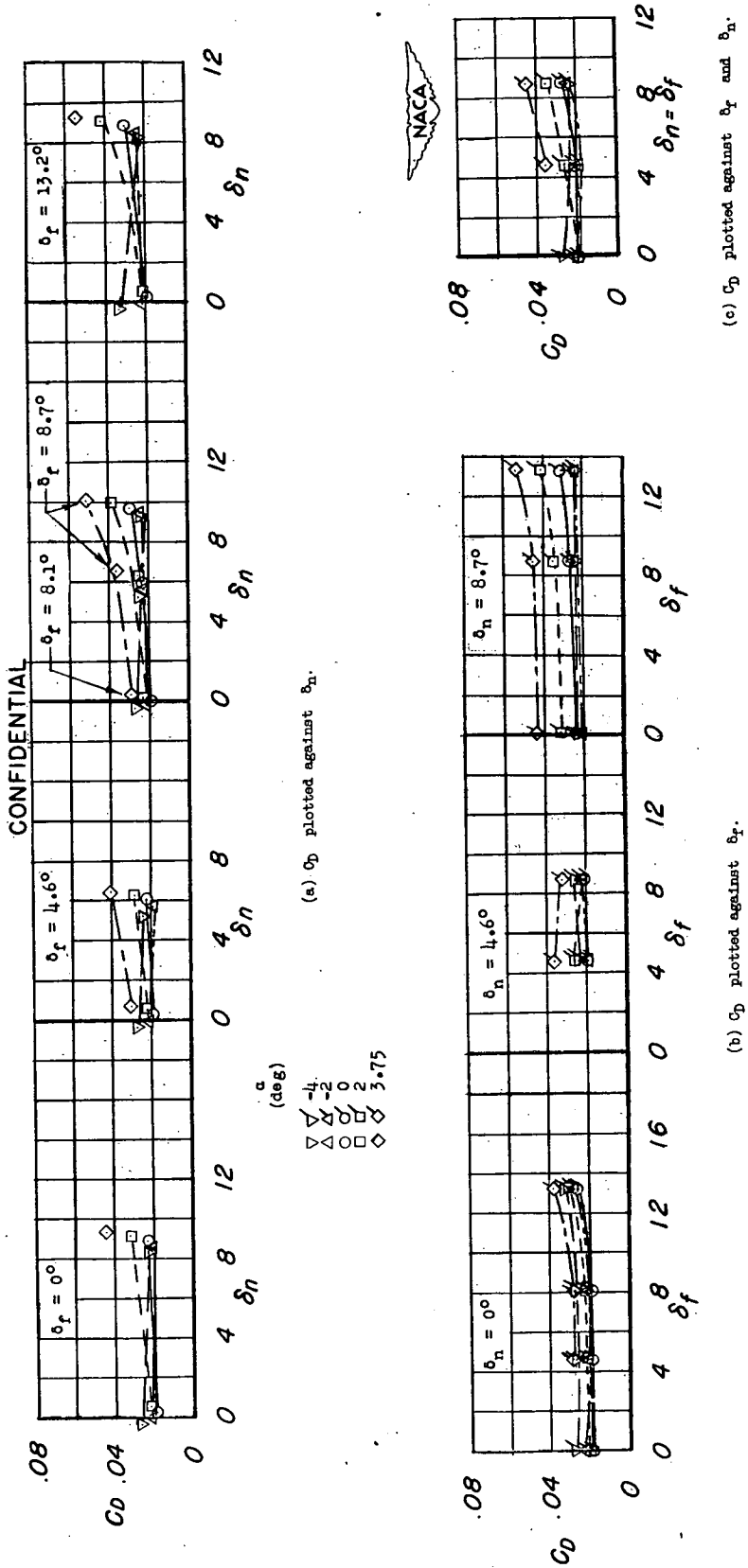

Figure 4.- Drag characteristics of flapped wing tested in the presence of a fuselage. R = 3.0 × 10^6; M = 1.9. Flagged symbols indicate modified test data.

CONFIDENTIAL

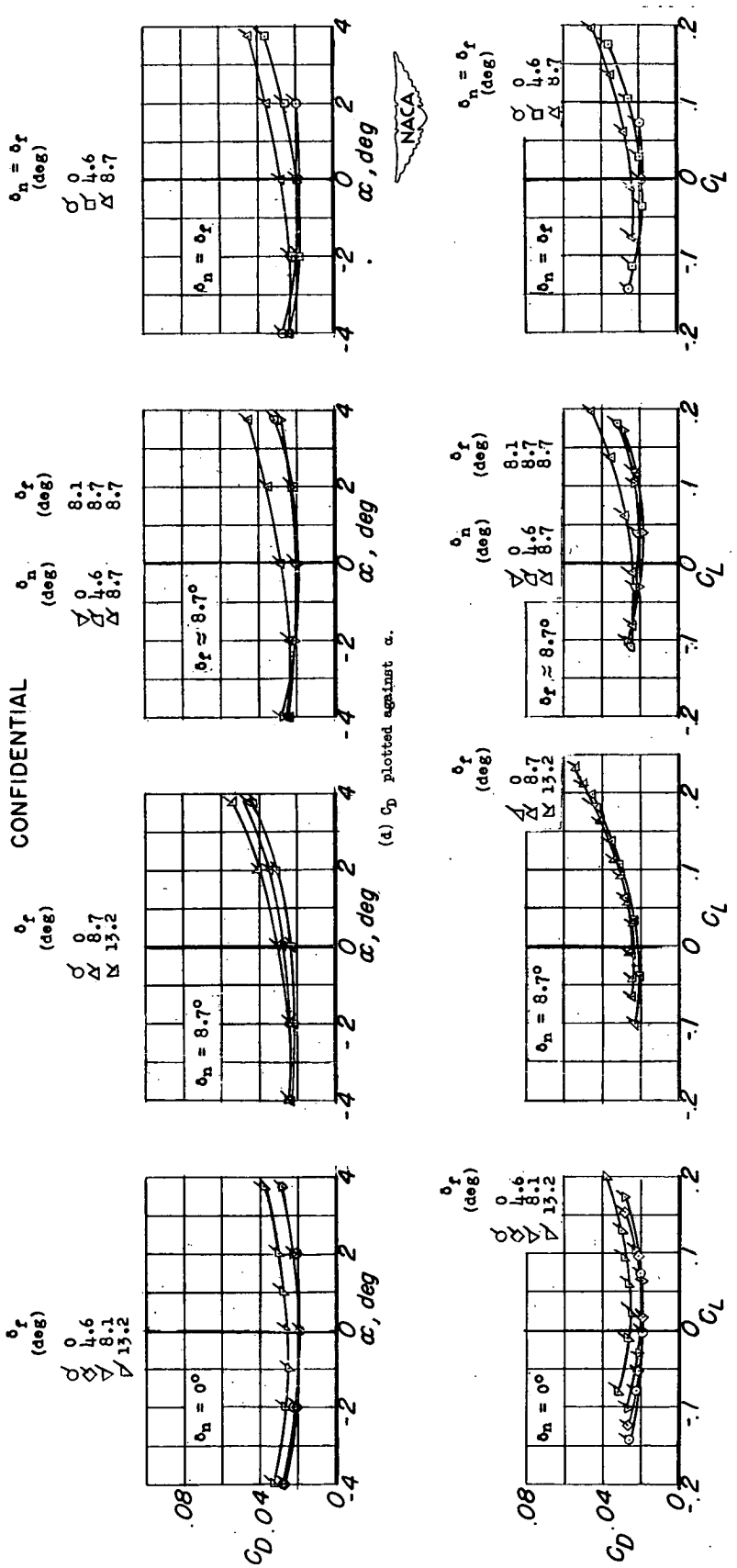

Figure 4.- Concluded.

CONFIDENTIAL

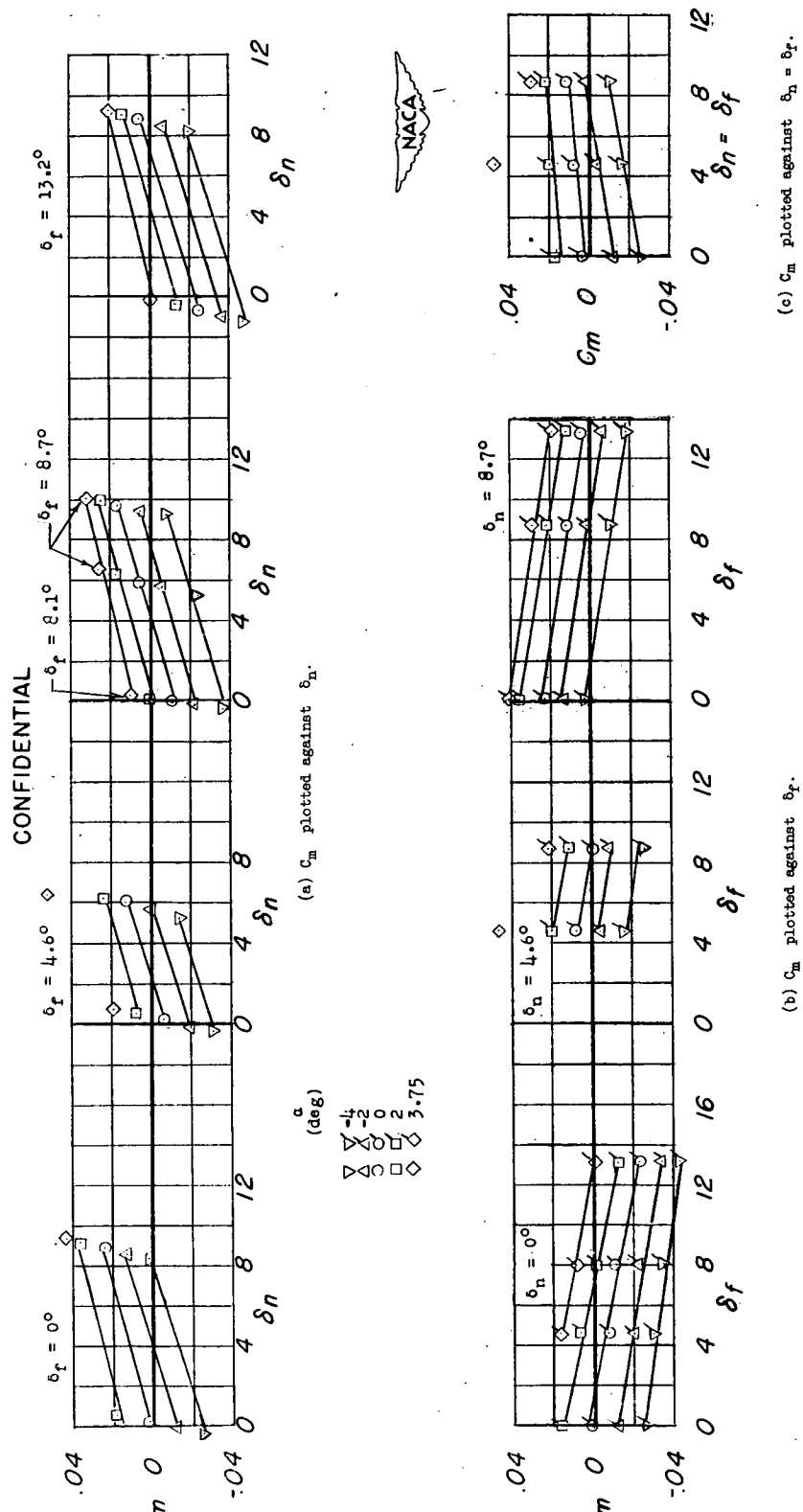

Figure 5.- Pitching-moment characteristics of a flapped wing tested in the presence of a fuselage. R = 3.0×10^6; M = 1.9. Flagged symbols indicate modified test data.

CONFIDENTIAL

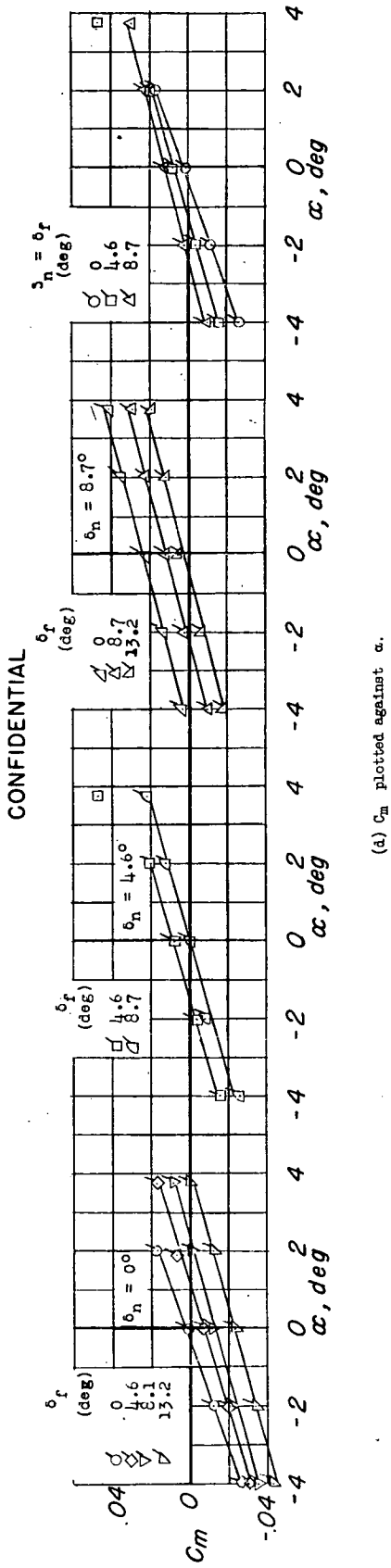

(d) C_m plotted against α.

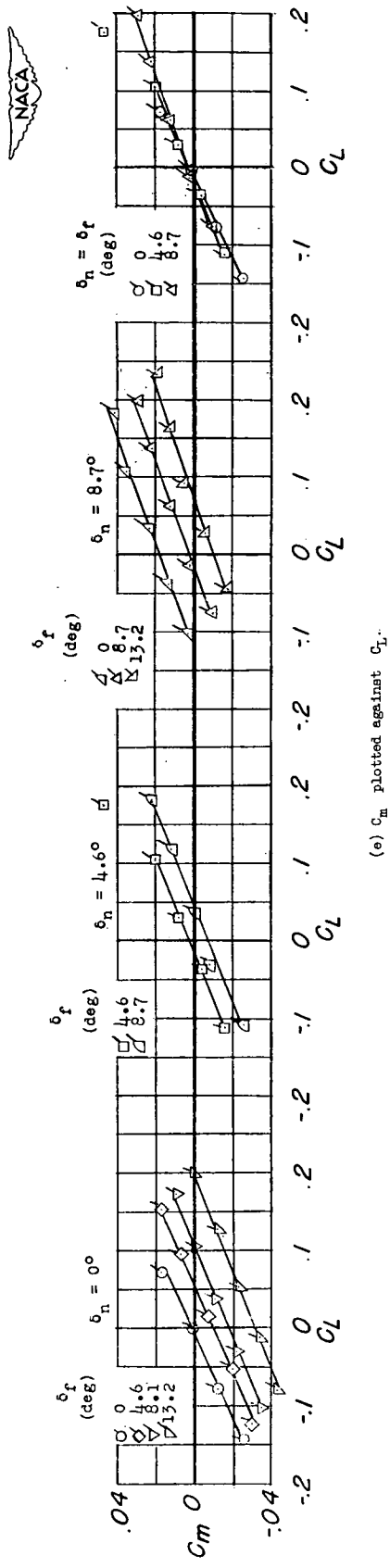

(e) C_m plotted against C_L.

Figure 5.- Concluded.

CONFIDENTIAL

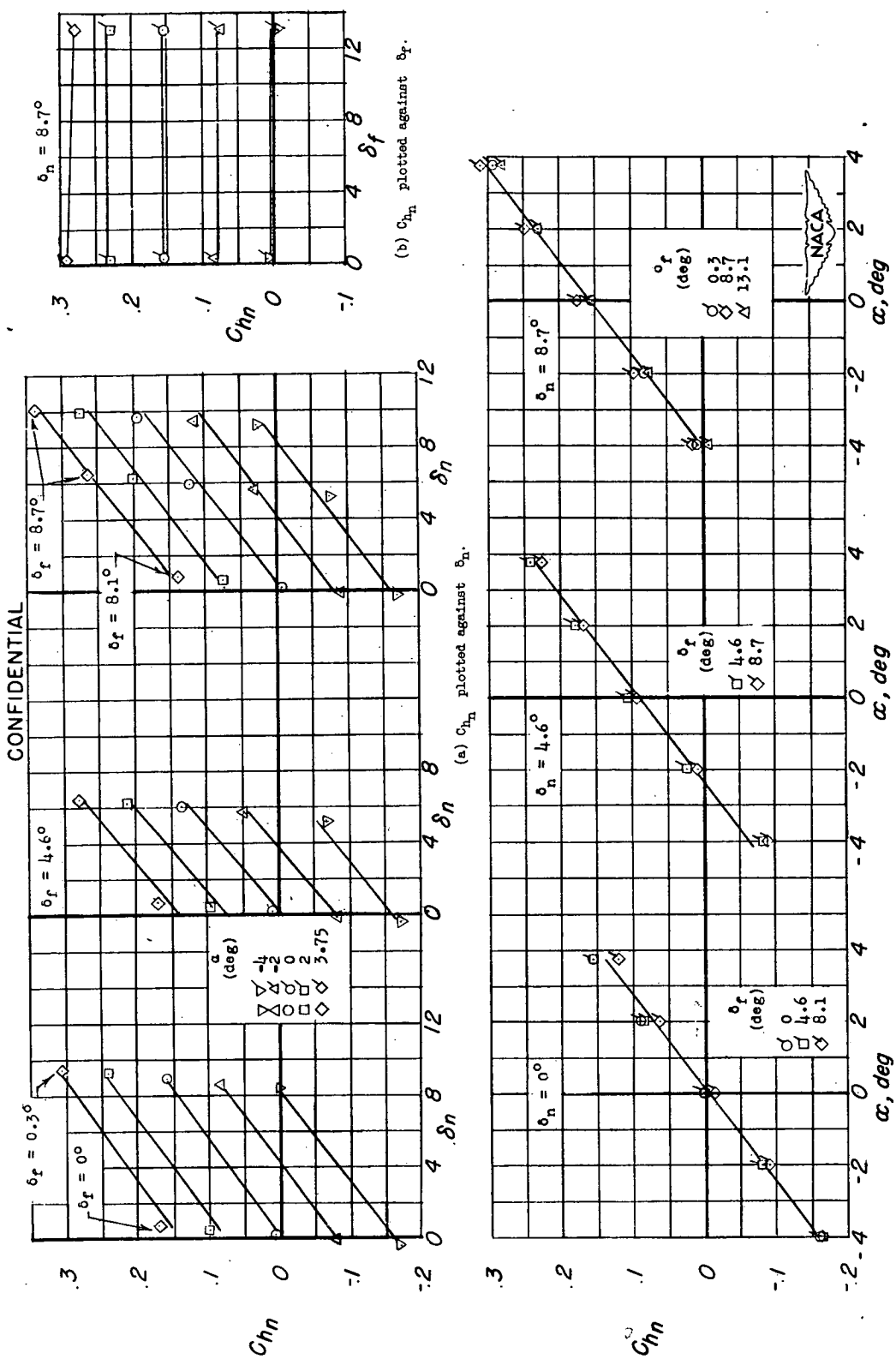

Figure 6.- Nose-flap hinge-moment characteristics for flapped wing tested in the presence of a fuselage. R = 3.0 × 10^6; M = 1.9. Flagged symbols indicate modified test data.

CONFIDENTIAL

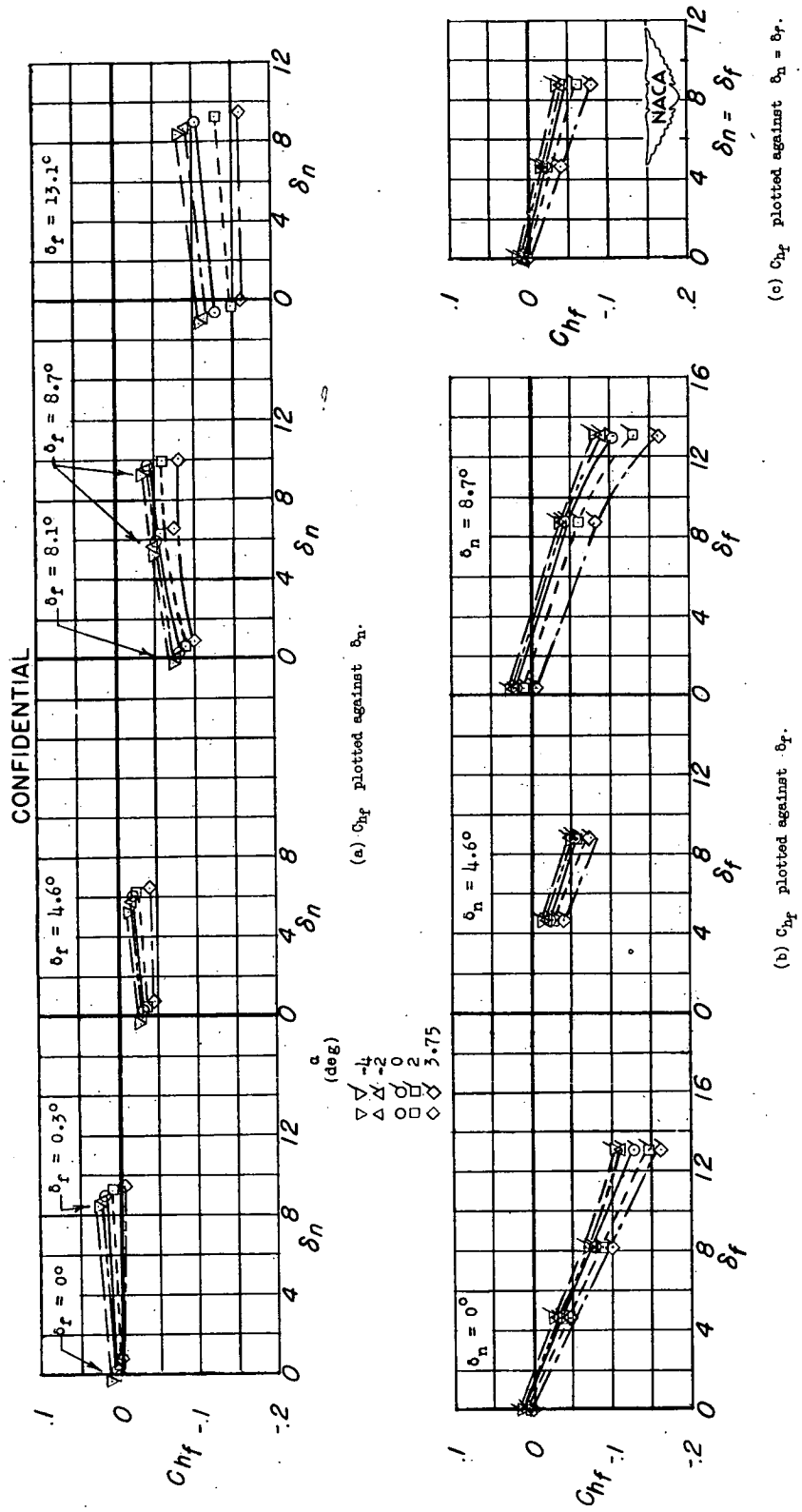

Figure 7.- Trailing-edge flap hinge-moment characteristics for flapped wing tested in the presence of a fuselage. R = 3.0×10^6; M = 1.9. Flagged symbols indicate modified test data.

CONFIDENTIAL

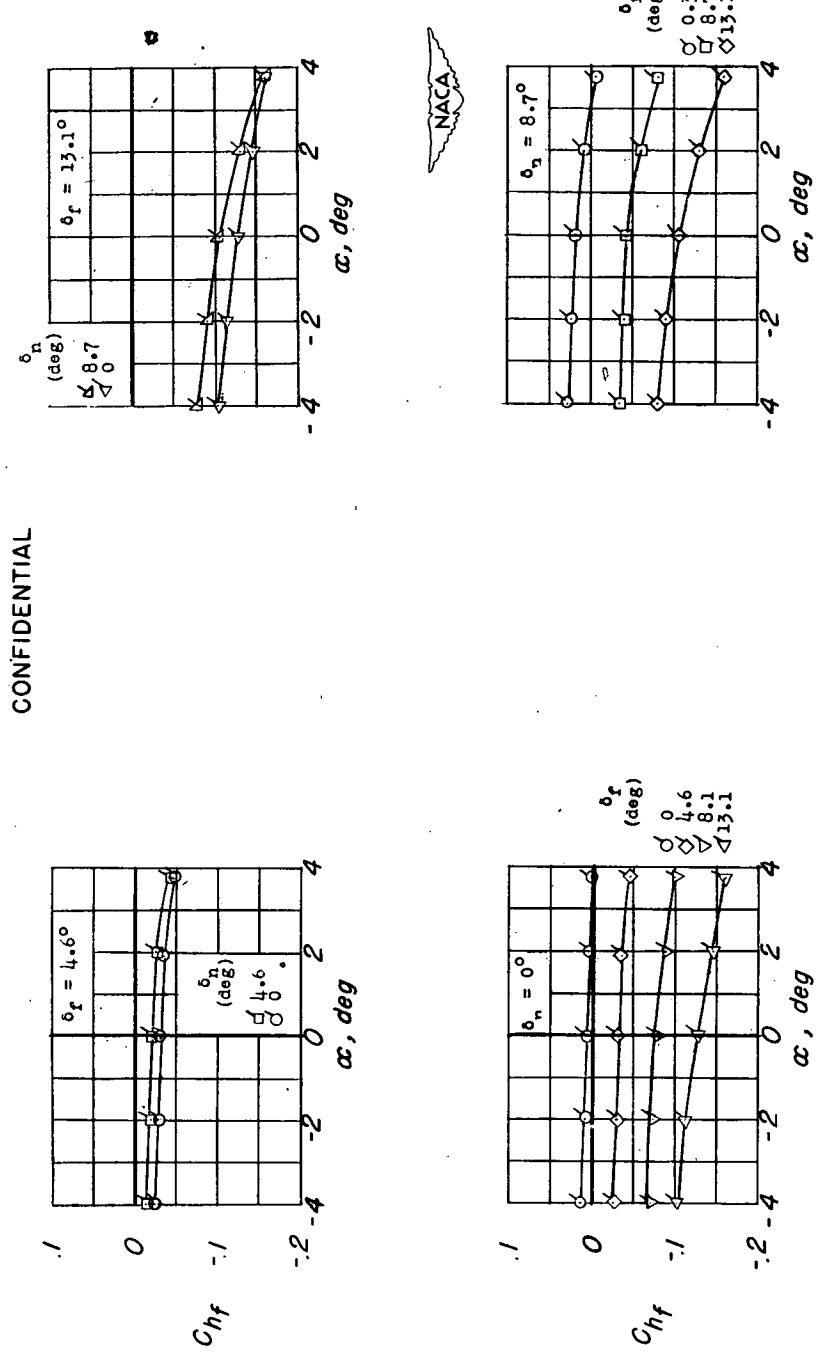

(a) C_{hf} plotted against α.

Figure 7.- Concluded.

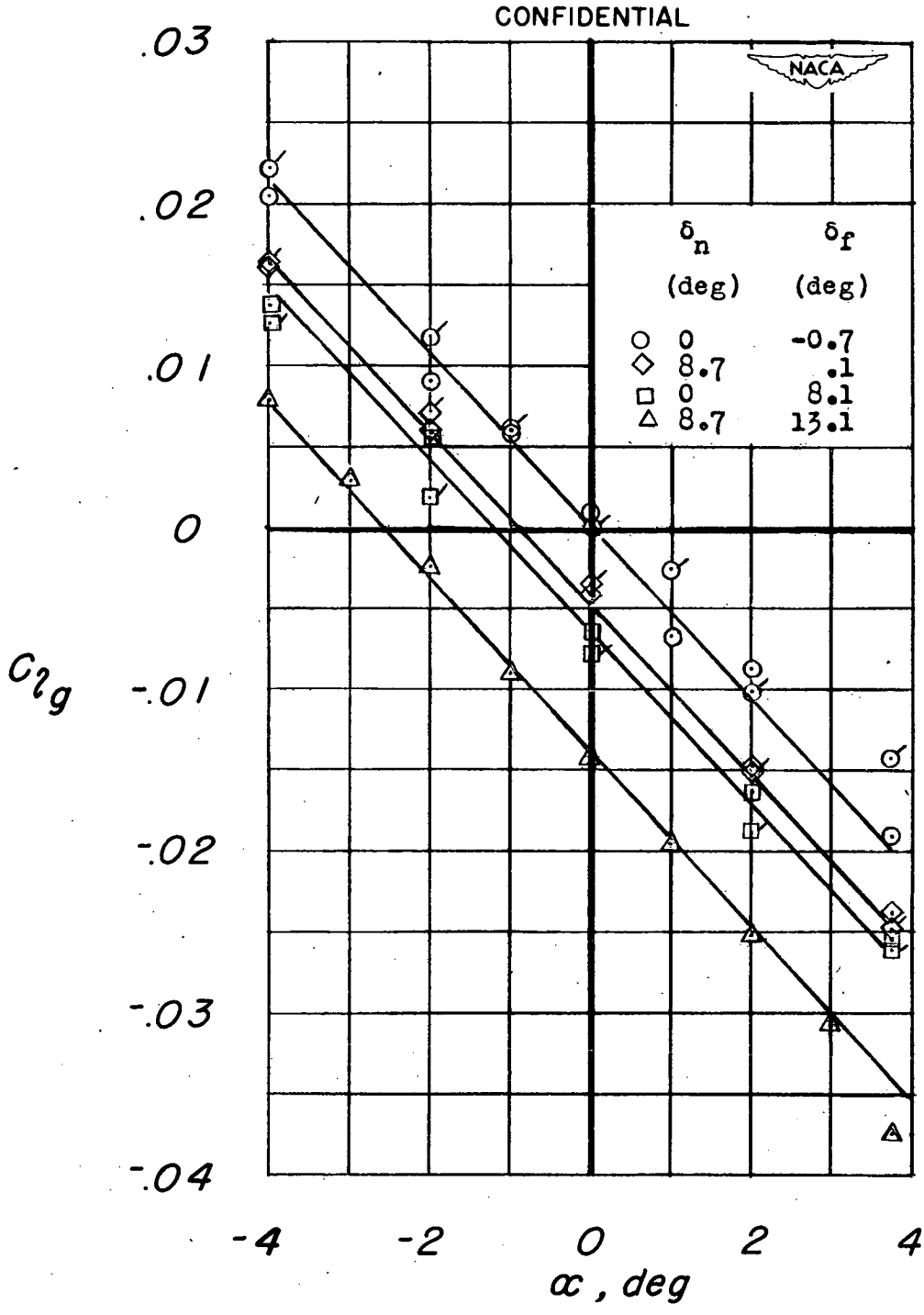

Figure 8.- Rolling-moment characteristics for flapped wing tested in the presence of a fuselage. $R = 3.0 \times 10^6$; $M = 1.9$. Flagged symbols indicate repeat runs. All symbols indicate modified test data.

CONFIDENTIAL

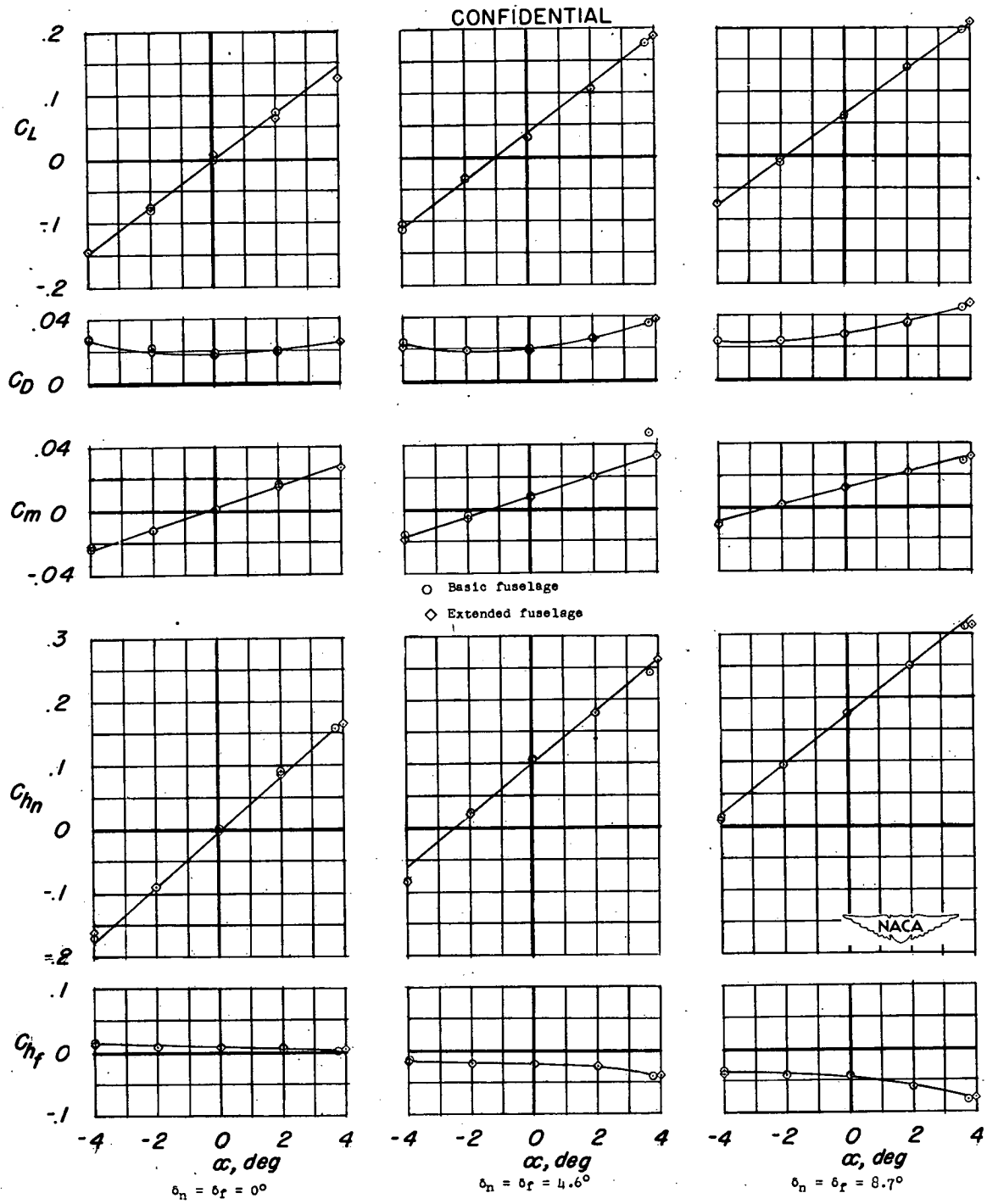

Figure 9.- Aerodynamic characteristics of a flapped wing tested at two locations along a fuselage. R = 3.0 × 10^6; M = 1.9. All symbols indicate modified test data.